Vortex penetration into a type II superconductor due to a mesoscopic external current

Eran Sela and Ian Affleck
Department of Physics and Astronomy, University of British Columbia, Vancouver, British Columbia, Canada V6T 1Z1
(Received 22 October 2008; published 7 January 2009)

Applying the London theory we study curved vortices produced by an external current near and parallel to the surface of a type II superconductor. By minimizing the energy functional we find the contour describing the hard core of the flux line and predict the threshold current for entrance of the first vortex. We assume that the vortex entrance is allowed due to surface defects, despite the Bean-Livingston barrier. Compared to the usual situation with a homogeneous magnetic field, the main effect of the present geometry is that larger magnetic fields can be applied locally before vortices enter the superconducting sample. It is argued that this effect can be further enhanced in anisotropic superconductors.

DOI: 10.1103/PhysRevB.79.024503 PACS number(s): 74.25.Ha, 74.25.Op, 74.25.Qt

I. INTRODUCTION

Surface-barrier effects in type II superconductors (SCs) were predicted by Bean and Livingston[1] and de Gennes.[2] The entry of flux lines into a planar type II superconductor situated in an external magnetic field H_{ext} parallel to its surface is opposed by a strong surface barrier when $H_{\text{ext}}=H_{c1}$, the first critical field. Therefore the entry of flux lines could occur at a field value $H_{\text{ext}}=H_S\sim H_{c2}\gg H_{c1}$, where H_{c2} is the second critical field. These surface-barrier effects have been observed experimentally in the 1960s on lead thallium alloys[3] and on niobium metal,[4] and make it difficult to measure directly the thermodynamic properties of the superconductor.

Typically surface barriers are reduced due to surface disorder, which creates large local magnetic fields and allows for nucleation of vortices. Suppression of surface barriers for flux penetration was observed on YBaCuO (Ref. 5) and in BiSrCaCuO whiskers[6] due to heavy-ion irradiation. In ellipsoid-shaped YBaCuO it has been argued that due to roughness of submicrometer order, the surface barrier does not push the penetration field H_S above H_{c1} but only lowers the rate of vortex entry.[7]

Another source for the delay of the entry of flux lines into superconductors is the "geometrical barrier,"[8,9] which is particularly important in thin films of constant thickness (i.e., rectangular cross section). This effect is absent only when the superconductor is of exactly ellipsoidal shape or is tapered like a wedge with a sharp edge where flux penetration is facilitated. The resulting absence of hysteresis in wedge-shaped samples was nicely shown by Morozov *et al.*[10]

In this paper we study another source for the delay of entrance of flux lines due to inhomogeneity of the external magnetic field. In particular we consider magnetic field produced by an external current I flowing parallel to the surface of a type II superconductor, see Fig. 1. The magnetic field produced by the external current enters the sample as curved vortices at sufficiently large current. We find that the entrance of the first line occurs when the induced magnetic field at the surface at the position closest to the wire already exceeds the bulk critical field H_{c1}. This delay in entrance of the curved vortices occurs due to geometrical reasons. The entry and outlet points are associated with an energy cost $\sim\frac{\phi_0^2}{\mu_0\lambda}$, where λ is the penetration depth, ϕ_0 is the flux quantum, and μ_0 is the free permeability. Note that $\phi_0^2/\mu_0k_B=0.2464\times10^6$ K μm, implying that in typical superconductors this is a large energy scale. In addition the spatially averaged magnetic field experienced by the vortex is lower than the maximal one occurring closest to the wire. Considering those effects in an actual calculation we find how large a magnetic field can be applied locally without introducing vortices into the sample.

This implies that application of magnetic field by an external current near the SC can be convenient for experiments, demanding sizable magnetic fields in the vortex-free state. As an example of such an experiment we mention the London-Hall effect.[11] Whereas this effect was observed in regular superconductors,[12–14] it is now interesting to measure it in high-temperature superconductors. Typically H_{c1} is quite low in these materials, and therefore vortices penetrate the sample at very low homogeneous magnetic fields; hence our geometry can be useful. However other surface effects seem to be an additional obstacle for the observation of the London-Hall effect in high-temperature superconductors.[15]

A parameter which we leave out of consideration in this work is the anisotropy of the superconductor, which is particularly important in high-temperature layered superconductors. In the case of strong anisotropy additional complications enter the problem even in the case of uniform magnetic field, where the direction of the vortices deviates

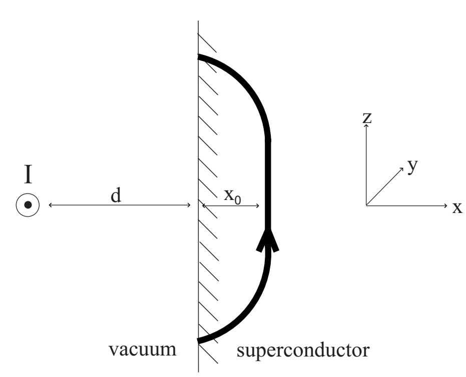

FIG. 1. Curved flux line near the surface of a superconductor enabled by an external current I.

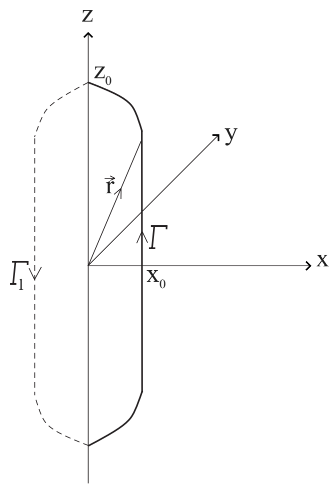

FIG. 2. Γ is the axial line of the vortex line. The closed contour γ is $\Gamma+\Gamma_1$.

from the direction of the external magnetic field.[16] For certain (elliptical) treatment of the short-distance cutoff the vortices can have two different directions, corresponding to two degenerate minima in the free energy.[17]

We argue that strong anisotropy is expected to have important effects in our geometry, increasing further the maximal local magnetic field allowed before curved flux lines penetrate the sample. Consider the case where the $\hat{c}$ axis of a uniaxially anisotropic superconductor corresponds to the direction $\hat{x}$ in our geometry, $\hat{c}\parallel\hat{x}$. In this case the surface of the superconductor, parallel to the external wire, corresponds to an ab plane. In the limit of strong anisotropy $\lambda_{ab}\ll\lambda_c$ the bulk critical field parallel to the surface $H_{c1}\cong\frac{\phi_0}{4\pi\mu_0\lambda_{ab}\lambda_c}\log\frac{\lambda_c}{\xi}$ becomes very small. On the other hand, the entry and outlet points of the flux line are associated with a large energy cost $\sim\frac{\phi_0^2}{\mu_0\lambda_{ab}}$ independent of λ_c. Therefore we expect the maximal surface magnetic field before the entry of the first vortex to increase relative to H_{c1} as a function of λ_c/λ_{ab}. We leave a detailed treatment of anisotropy in this geometry for future work.

This paper is organized as follows. In Sec. II we formulate the problem and obtain expressions for the magnetic field and free energy within the London theory. In Sec. III we present and discuss the numerical results for the minimization of the free energy as a function of vortex contour. In Secs. II and III A we consider the simpler but unrealistic case of a wire with zero width (i.e., $\ll\lambda$). In Sec. III B we generalize to wires with finite width. Section IV contains conclusions. Some details about the derivation of the free energy are relegated to the Appendix.

II. FORMULATION

Suppose that a type II SC occupies the region $x>0$ and magnetic field is induced by an external current I flowing along a wire of zero cross section at $(x,z)=(-d,0)$, see Fig. 1. Our main object under consideration is a curved flux line lying in the plane $y=0$. Let γ denote the closed contour in Fig. 2 consisting of the axial line of the flux line Γ and a line Γ_1 symmetric to Γ with respect to the plane $x=0$, corresponding to an image vortex. Upon further increasing the current a lattice of curved vortices is expected to form along the wire. However here we shall concentrate on small currents and a single flux line.

In the type II limit, where the coherence length ξ is much shorter than the penetration depth λ, the total free energy at zero temperature is given by[2]

$$F[\Gamma]=\frac{\mu_0}{2}\int_{r>\xi}d^3r[\vec{H}^2+\theta(x)\lambda^2(\vec{\nabla}\times\vec{H})^2]-\mu_0\int d^3r\vec{A}\cdot\vec{j}_{\text{ext}}. \tag{1}$$

Here $\vec{j}_{\text{ext}}=-I\delta(x+d)\delta(z)\hat{y}$, I is the applied current through the wire, $\vec{A}$ is the vector potential $\vec{H}=\vec{\nabla}\times\vec{A}$, and $\theta(x)$ is the unit step function. The integral $\int_{r>\xi}$ is carried out in all space outside of the vortex "hard core" Γ. We assume that the radius of curvature of Γ is larger than ξ at any point in Γ. Note that at $x=0$ there is an apparent kink in γ; however this should be thought of as a kink only for length scales that are large compared to ξ.

The corresponding equations for the magnetic field $\vec{H}$ are the Maxwell equation, $\vec{\nabla}\times\vec{H}=\vec{j}_{\text{ext}}$ for $x<0$, and the London equation, $(1-\lambda^2\vec{\nabla}^2)\vec{H}(\vec{r})=\frac{\phi_0}{\mu_0}\int_\Gamma d\vec{r}'\,\delta^3(\vec{r}-\vec{r}')$ for $x>0$. For all x we also have $\vec{\nabla}\cdot\vec{H}=0$. In addition we impose appropriate boundary conditions at $x=0$; the magnetic field is continuous, and no supercurrent flows perpendicular to the surface, $\vec{j}_x=(\vec{\nabla}\times\vec{H})_x=0$. To construct a solution we use the functions

$$\vec{H}^{\text{hom}}_{A(\vec{k}_2),B(\vec{k}_2)}(\vec{r})=\int\frac{d^2k_2}{(2\pi)^2}e^{i\vec{k}_2\cdot\vec{r}}\times\begin{cases}A(\vec{k}_2)[-k_2^2\hat{x}+i\vec{k}_2\tau(k_2)]e^{-\tau(k_2)x} & x>0,\\ B(\vec{k}_2)[k_2\tau(k_2)\hat{x}+i\vec{k}_2\tau(k_2)]e^{k_2x} & x<0,\end{cases}$$

$$\vec{H}_\gamma(\vec{r})=\frac{\phi_0}{\mu_0}\int_\gamma d\vec{r}'\int\frac{d^3k}{(2\pi)^3}e^{i\vec{k}\cdot(\vec{r}-\vec{r}')}\frac{1}{1+\lambda^2k^2},$$

$$\vec{H}_{I',d'}(\vec{r})=\frac{I'}{2\pi}\frac{(-z,0,x+d')}{(x+d')^2+z^2}. \tag{2}$$

Here $\vec{k}_2=k_y\hat{y}+k_z\hat{z}$, $k_2=\sqrt{k_y^2+k_z^2}$, and $\tau(k)=\sqrt{k^2+\lambda^{-2}}$. For any $A(\vec{k}_2),B(\vec{k}_2)$, the function $\vec{H}^{\text{hom}}$ satisfies the homogeneous equations $\vec{\nabla}\times\vec{H}^{\text{hom}}=0$ for $x<0$ and $(1-\lambda^2\vec{\nabla}^2)\vec{H}^{\text{hom}}=0$ for $x>0$. The function $\vec{H}_\gamma$ satisfies the London equation $(1-\lambda^2\vec{\nabla}^2)\vec{H}_\gamma(\vec{r})=\frac{\phi_0}{\mu_0}\int_\gamma d\vec{r}'\,\delta^3(\vec{r}-\vec{r}')$ in all space. The function $\vec{H}_{I',d'}$ satisfies Maxwell equation $\vec{\nabla}\times\vec{H}_{I',d'}(\vec{r})=\vec{j}'_{\text{ext}}$ for $\vec{j}'_{\text{ext}}=I'\delta(x+d')\delta(z)\hat{y}$ for all space.

Defining the surface two-dimensional Fourier transform $\vec{H}^{\text{surf}}_\mu(\vec{k}_2)=\int dydz e^{-i\vec{k}_2\cdot\vec{r}}\vec{H}_\mu(0,y,z)$ for $\mu=\gamma,\{I',d'\}$, one finds

$$\vec{H}^{\text{surf}}_\gamma(\vec{k}_2)=\frac{\phi_0}{2\mu_0\lambda^2}\int_\gamma d\vec{r}'e^{-i\vec{k}_2\cdot\vec{r}'}\frac{e^{-\tau(k_2)|r'_x|}}{\tau(k_2)},$$

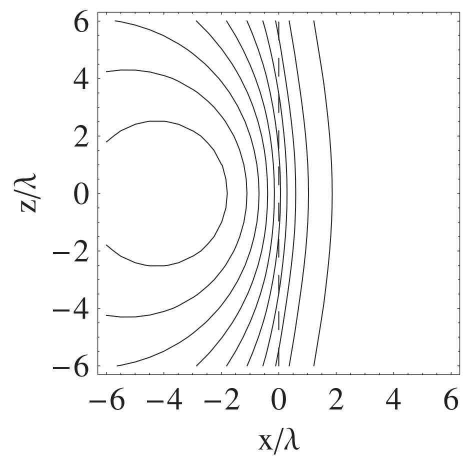

FIG. 3. Field lines of the vortex-free solution $\vec{H}_0(x,z)$ for $d=5\lambda$ [direction of field lines corresponds to anticlockwise rotation around $(x,z)=(-d,0)$].

$$\vec{H}^{\mathrm{surf}}_{I,d}(\vec{k}_2) = \delta(k_y)\pi I e^{-|k_z d|}(i\ \mathrm{sgn}\ k_z, 0, \mathrm{sgn}\ d). \tag{3}$$

The solution of the equations satisfying the desired boundary conditions is obtained by adding together the functions in Eq. (2) and solving for $A(\vec{k}_2)$ and $B(\vec{k}_2)$ to give continuity. It is convenient to include an image current at $x=-d$. The total magnetic field is

$$\vec{H} = \vec{H}_0 + \vec{H}_v + \vec{H}_s,$$

$$\vec{H}_0 = \theta(-x)(\vec{H}_{I,d} + \vec{H}_{-I,-d}) + \vec{H}_{s0}, \quad \vec{H}_{s0} = \vec{H}^{\mathrm{hom}}_{A_0,B_0},$$

$$\vec{H}_v = \theta(x)\vec{H}_\gamma, \quad \vec{H}_s = \vec{H}^{\mathrm{hom}}_{A_1,B_1}, \tag{4}$$

where

$$A_0(\vec{k}_2) = \frac{2[\vec{H}^{\mathrm{surf}}_{I,d}(\vec{k}_2)]_z}{ik_z[\tau(k_2)+k_2]}, \quad B_0(\vec{k}_2) = -A_0(\vec{k}_2)\frac{k_2}{\tau(k_2)},$$

$$A_1(\vec{k}_2) = B_1(\vec{k}_2) = \frac{[\vec{H}^{\mathrm{surf}}_\gamma(\vec{k}_2)]_x}{k_2[k_2+\tau(k_2)]}. \tag{5}$$

In the absence of vortices the magnetic field is given by $\vec{H}_0$. It is plotted in Fig. 3 for $d=5\lambda$.

The total free energy as function of Γ is obtained by substituting the magnetic field Eq. (4) into the free energy Eq. (1). We obtain

$$F = F_0 + F_v + F_s + F_{\mathrm{ext}}. \tag{6}$$

Here

$$F_0 = \frac{\mu_0}{2}\int d^3r[\vec{H}_0^2 + \theta(x)\lambda^2(\vec{\nabla}\times\vec{H}_0)^2 - 2\vec{A}_0\cdot\vec{j}_{\mathrm{ext}}],$$

$$F_i = \frac{\mu_0}{2}\int d^3r[\vec{H}_i^2 + \theta(x)\lambda^2(\vec{\nabla}\times\vec{H}_i)^2], \quad i=v,s,$$

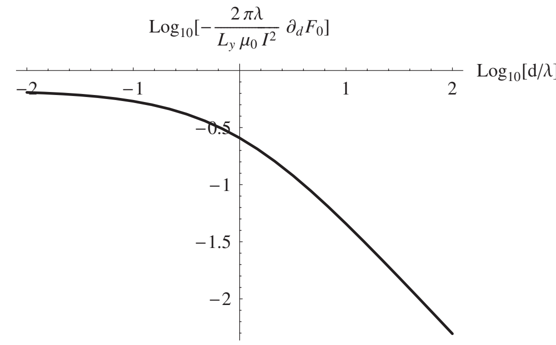

FIG. 4. Repulsive force between the superconductor and the wire in the absence of vortices. The dimensionless force $-(2\pi\lambda/L_y\mu_0 I^2)\partial_d F_0$ behaves as $\lambda/(2d)$ for $d\gg\lambda$ and goes to a constant $c_0\sim 0.665$ for $d\ll\lambda$.

$$F_{\mathrm{ext}} = -\mu_0\int d^3r(\vec{A}_v+\vec{A}_s)\cdot\vec{j}_{\mathrm{ext}}. \tag{7}$$

Here $\vec{H}_i=\vec{\nabla}\times\vec{A}_i$ $(i=0,v,s)$. All mixed terms between $\vec{H}_0,\vec{H}_v,\vec{H}_s$ vanish. For the vanishing of mixed terms involving $\vec{H}_v$, see p. 579 of Ref. 18. We prove the vanishing of the remaining crossed terms between $\vec{H}_0$ and $\vec{H}_s$ in the Appendix.

The term F_0 is the energy of the system without vortices. To evaluate it we introduce a finite wire radius $a\ll\lambda,d$ and assume that the external current flows in a thin shell of this radius. Note that F_0 scales linearly with the length of the wire, L_y. The result of a calculation, using the methods of the Appendix, is

$$\frac{F_0}{L_y} = -\frac{\mu_0 I^2}{2\pi}\left[\frac{1}{2}\log(2d/a) + g(d/\lambda)\right],$$

$$g(y) = \int_0^\infty dx\frac{e^{-2x}}{x+\sqrt{x^2+y^2}}. \tag{8}$$

We can infer from it the repulsive force per unit length $\frac{\partial_d F_0}{L_y}<0$ between the wire and the SC. It is plotted in Fig. 4 (for $a/\lambda=0.01$). Using $g(y\to\infty)=\frac{1}{2y}$ and $g(y\to 0)=\frac{1}{2}\log\frac{1}{2y}$, we may identify two regimes. (i) $d\gg\lambda$: here $g\to 0$ and $\frac{\partial_d F_0}{L_y}\to-\frac{\mu_0 I^2}{2\pi(2d)}$. In agreement with Ampere force law, this corresponds to a repulsive force per unit length between two wires that are $2d$ apart carrying current I with opposite direction. This is the origin of the levitation effect. The second wire corresponds to the image term $\vec{H}_{-I,-d}$ in Eq. (4). (ii) $d\ll\lambda$: the $1/d$ divergence in the force is cutoff by λ. The limiting repulsion force per unit length as the wire approaches the surface is $\frac{\partial_d F_0}{L_y}\to-\frac{\mu_0 I^2}{2\pi\lambda}c_0$ where $c_0\cong 0.665$.

The term F_{ext} accounts for the interaction between the vortex and the external current. Using $\vec{j}_{\mathrm{ext}}=-I\delta(x+d)\delta(z)\hat{y}$ we have

$$F_{\rm ext} = \mu_0 I \int_{-\infty}^{\infty} dy[\vec{A}_v(-d,y,0) + \vec{A}_s(-d,y,0)]_y. \quad (9)$$

The contour of integration $(x,y,z)=(0,-\infty,0)\to(0,\infty,0)$ corresponds to the external current. Physically the wire should be closed into a loop, and we may close the contour of integration, e.g., in the xy plane from $x\to-\infty$. Then, using the Green's theorem we obtain

$$F_{\rm ext} = \mu_0 I \int_{-\infty}^{-d} dx \int_{-\infty}^{\infty} dy[\vec{H}_v(x,y,0) + \vec{H}_s(x,y,0)]_z.$$

Note that $\vec{H}_v(x,y,0)$ vanishes at $x<0$. Using the formula for $\vec{H}_s$, Eq. (4), we obtain

$$F_{\rm ext} = -\frac{I\phi_0}{\pi}\int_\Gamma d\vec{r}_z \int_0^\infty dk e^{-kd}\cos(kr_z) \times (1-e^{-\tau(k)r_x})\left(1-\frac{k}{\tau(k)}\right). \quad (10)$$

We used the identity $\oint_\gamma d\vec{r}\cdot\vec{\nabla}\mathcal{F}(\vec{r})=0$ which holds for any continuous function $\mathcal{F}$ and closed contour γ. In this calculation $\mathcal{F}(\vec{r})=e^{ikr_z}\,\mathrm{sgn}(r_x)(1-e^{-\tau(k)|r_x|})$.

The terms F_v and F_s have been derived in Refs. 18 and 19,

$$F_v = \frac{\phi_0^2}{2\mu_0}\sum_{i=x,y,z}\int_\gamma d\vec{r}_i \int_\gamma d\vec{r}_i' \frac{\exp(-|\vec{r}-\vec{r}'|/\lambda)}{8\pi\lambda^2|\vec{r}-\vec{r}'|},$$

$$F_s = \frac{\phi_0^2}{2\mu_0}\int_\Gamma d\vec{r}_z \int_{\Gamma_1} d\vec{r}_z' V^{(s)}(\vec{r}-\vec{r}'). \quad (11)$$

The term F_v is sensitive to the short-distance cutoff ξ. To account for the cutoff we restrict the contour integration to $|\vec{r}-\vec{r}'|>\xi$. The anisotropic kernel for F_s is

$$V^{(s)}(\vec{r}) = \frac{1}{2\pi\lambda^2}\int_0^\infty dk\left(1-\frac{k}{\tau(k)}\right)e^{-\tau(k)|r_x|}J_0(k|r_z|),$$

where $J_0(x)$ is a Bessel function, and this integral can be done and expressed in terms of other Bessel functions.[19] Note that $V^{(s)}(r_x\to0,r_z\to0)=(2\pi\lambda^3)^{-1}$, hence there is no need to regulate F_s with a cutoff.

Different than the usual case with a uniform magnetic field, in our problem the energy $F=F_0+F_v+F_s+F_{\rm ext}$ is a function of the contour Γ and is minimized for a particular contour which we need to find. To this end we minimize $F[\Gamma]$ numerically, approximating Γ by a polyline having $2M$ equal length sides ($M=8$ in most simulations). We assume that Γ has the reflection symmetry $z\to-z$. This leads to a $M+1$-dimensional parameter space in which we search for the minimum of F. For an example see Fig. 5. In all our calculations $\xi=.001\lambda$.

III. SURFACE BARRIER

We find that the free energy contains a surface energy barrier. From this section we shall disregard the vortex-independent term of the free energy, $F\to F_v+F_s+F_{\rm ext}$. For later comparison we briefly discuss the case with homogeneous magnetic field.[1] Consider a semi-infinite type II superconductor with a flux thread within it and parallel to the surface and to the external magnetic field $H_{\rm ext}$ ($\|\hat{z}$). The line energy $f=F/L_z$ (L_z is the length of the vortex taken to be parallel to $\hat{z}$) as a function of the distance from the surface x_0 is given by[1,2]

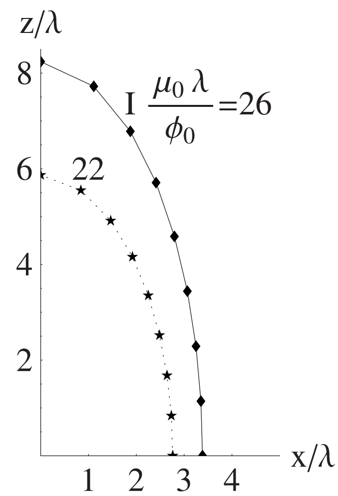

FIG. 5. Contours corresponding to a local minimum of F for $d=10\lambda$ and for the specified currents. We assume that Γ has the reflection symmetry $z\to-z$ and plot Γ only for $z\geq0$.

$$f(x_0) = \phi_0\left[H_{\rm ext}e^{-x_0/\lambda} - \frac{1}{2}h(2x_0) + H_{c1} - H_{\rm ext}\right]. \quad (12)$$

Here $h(r)=\frac{\phi_0}{2\pi\mu_0\lambda^2}K_0(\frac{r}{\lambda})$ is the function giving the field at distance r of a single straight flux line, $H_{c1}=\frac{1}{2}h(\xi)\cong\frac{\phi_0}{4\pi\mu_0\lambda^2}\log\frac{\lambda}{\xi}$, and K_0 is the zero-order Bessel function. The term $\propto e^{-x_0/\lambda}$ describes the repulsive interaction of the line with the external field and associated screening currents. The term $\propto h(2x_0)$ represents the attraction between the line and its image. When $H_{\rm ext}\sim H_{c1}$ there is a strong barrier opposing the entry of a line. We can understand this barrier as follows. When $H_{\rm ext}=H_{c1}$, $f(x_0=0)=f(x_0=\infty)=0$. If we start from large x_0 and bring the line closer to the surface, the repulsive term ($\sim e^{-x_0/\lambda}$) dominates the image term $[h(2x_0)\sim e^{-2x_0/\lambda}]$. Thus f becomes positive and we have a barrier. The barrier disappears, however, in high fields. When $H_{\rm ext}>H_S=\phi_0/4\pi\lambda\xi$, the slope $\partial f/\partial x_0|_{x_0\sim\xi}$ becomes negative. H_S is of the order of the thermodynamic critical field H_{c2}. The conclusion is that at field $H_{\rm ext}<H_S$, the lines cannot enter in an ideal specimen (although their entry is thermodynamically allowed as soon as $H_{\rm ext}>H_{c1}$). However this picture is modified in experiment due to surface inhomogeneities producing local large magnetic fields and allowing vortices to enter the sample above H_{c1}.

A. Results for wire with zero width

We find a similar energy barrier for the entrance of a curved vortex in our geometry with an external current rather

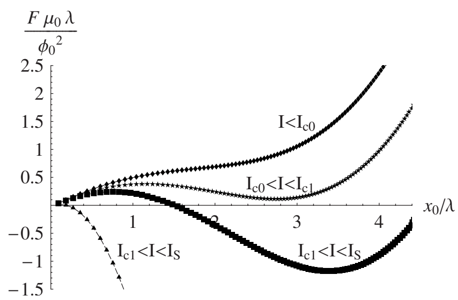

FIG. 6. Evolution of surface barrier as a function of external current for $d/\lambda=10$. When $I<I_{c0}$ (diamonds, $I=19\frac{\phi_0}{\mu_0\lambda}$) the force on the line always points toward the surface. When $I_{c0}<I<I_{c1}$ (stars, $I=22\frac{\phi_0}{\mu_0\lambda}$) there exists a metastable minima with positive energy. When $I_{c1}<I<I_S$ (squares and triangles $I=26,80\times\frac{\phi_0}{\mu_0\lambda}$) the minimum energy is negative, but a barrier opposes the entry of the flux line. Each point in this plot is obtained by minimizing F with respect to the contour Γ with a constraint of fixed x_0.

than a homogeneous external magnetic field. This barrier can be visualized in Fig. 6. Note that typically the barrier height Δ is of the order $\Delta\sim\phi_0^2/\mu_0\lambda\gg T_c$, where T_c is the critical temperature of the SC. This implies rather small tunneling probabilities $e^{-\Delta/T}\ll 1$ which prevent entry of vortices for clean surfaces. However for strong disorder, vortices can enter more efficiently via nucleation at impurity sites. The contours corresponding to the minimum of the curves with stars and squares in Fig. 6 are plotted in Fig. 5.

Figure 6 implies the following generic picture. For infinitesimal current there is no stable vortex configuration. As the current increases we identify three threshold currents $I_{c0}<I_{c1}<I_S$. When the current exceeds I_{c0} a metastable minima with $F>0$ occurs. When the current exceeds I_{c1}, the minimum energy changes sign, $F<0$, but still there is an energy barrier for the entrance of a flux line. When the current exceeds I_S the barrier disappears.

In Fig. 7 we investigated the dependence of I_{c0} and I_{c1} on the distance to the wire d. In the limit $d\gg\lambda$, $I_{c1}\to\pi dH_{c1}$, see diagonal dashed line. In that limit the region of metastability $I_{c0}<I<I_{c1}$ is very narrow. This behavior appears in sharp contrast to the case of uniform magnetic field even in the limit $d\gg\lambda$. Equation (12) predicts metastable solutions for infinitesimal homogeneous magnetic field H_{ext}. These metastable solutions live far from the surface as H_{ext} becomes smaller. This effect is absent in our geometry both due to the decay of the effective external magnetic field created by the wire at long distances from the surface and due to the line energy for penetration a long distance into the SC. In the other extreme limit $d\ll\lambda$ we observed from the numerical solution that the contour γ can be approximated by a circle centered at the origin. Making this assumption we can calculate $I_{c0}^{\text{circle}}=10^{0.6981}\frac{\phi_0}{\mu_0\lambda}$ ($x_0\sim 0.72\lambda$, $F\mu_0\lambda/\phi_0^2=0.1715$) and $I_{c1}^{\text{circle}}=10^{0.749}\frac{\phi_0}{\mu_0\lambda}$ ($x_0=1.27\lambda$, $F=0$) in the limit $d\to 0$. This approximation is in reasonable agreement with the actual solution as the horizontal dashed lines show.

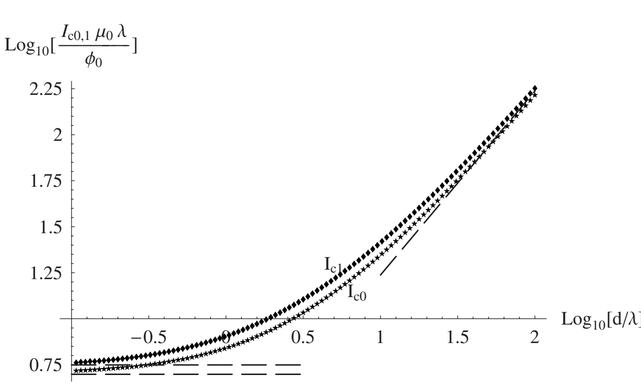

FIG. 7. Dependence of threshold currents I_{c0} and I_{c1} on d/λ.

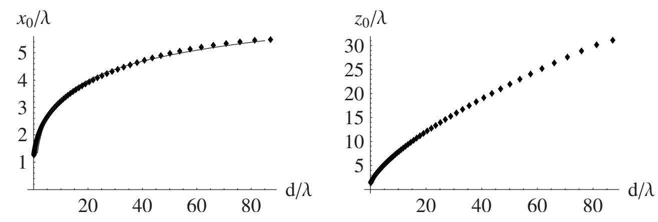

FIG. 8. Extensions of the curved flux line along x and z as a function of d/λ at $I=I_{c1}$.

The contour Γ changes as function of d. In Fig. 8 we plot the extension of the contour in the x and z directions. We fitted the numerical results for x_0 with an empirical formula $x_0/\lambda=c+\log(d/\lambda)$ with $c\sim 1$, implying that the penetration of the vortex is of order λ for all d. On the other hand it appears that z_0 grows linearly as a function of d. In the limit $d\to 0$ we have $x_0/\lambda\to 1.26$ and $z_0/\lambda\to 1.43$.

For disordered surfaces, the present geometry can be useful for application of large magnetic fields on a SC sample in a vortex-free state. The maximal magnetic field that can be applied in a vortex-free state using the wire geometry is $H_{\text{surface}}\equiv[\vec{H}_0]_z(x=z=0)|_{I\to I_{c1}}=[\vec{H}_{s0}]_z(0^+,0,0)|_{I\to I_{c1}}$ [see Eq. (4)] at $I\to I_{c1}$. In the limit $d\gg\lambda$, H_{surface} coincides with the bulk first critical field $H_{c1}\approx\frac{\phi_0}{4\pi\mu_0\lambda^2}\log(\lambda/\xi)$; however H_{surface} increases at smaller d, see Fig. 9. Note that the field enhancement is small for $d>3\lambda$ ($H_{\text{surface}}\cong 2H_{c1}$ for $d=3\lambda$).

We turn to an estimation of the threshold current I_S at which the barrier disappears. A more precise calculation would involve the Ginzbur-Landau theory. We follow the above analysis of H_S.[2] Since the London theory is applicable at distances $\gg\xi$ we estimate I_S using

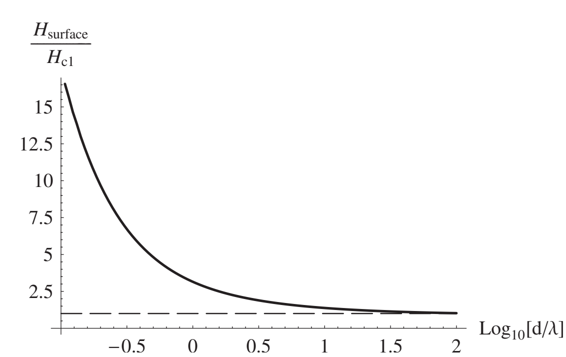

FIG. 9. Magnetic field at the surface just before the entry of the first vortex for $I\to I_{c1}$ (see definition of H_{surface} in text). At $d\gg\lambda$, $H_{\text{surface}}\to H_{c1}$. As d becomes smaller the SC can sustain larger magnetic fields in the vortex-free (Meissner) state.

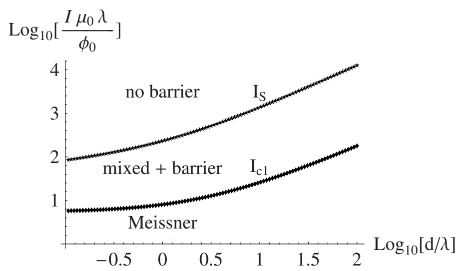

FIG. 10. Phase diagram. For $I<I_{c1}$ vortices are thermodynamically unfavorable. For $I>I_{c1}$ curved flux lines become favorable, but an energy barrier opposes their entry until the current exceeds I_S. A metastable phase exists in a narrow strip below the boundary $I=I_{c1}$, as shown in Fig. 7.

$$\left.\frac{\partial F}{\partial x_0}\right|_{x_0\sim\xi}=0. \tag{13}$$

We find numerically that at $x_0\ll\lambda$ the closed contour γ is well approximated by a circle with radius x_0 centered at $x=z=0$. In the limit $x_0\sim\xi\ll\lambda$ we can evaluate the functional $F(x_0)$ analytically. In Eq. (11) for F_v we can set $\exp(-|\vec{r}-\vec{r}'|/\lambda)\to 1$, hence

$$F_v(x_0)\sim\frac{\phi_0^2 x_0}{32\pi\mu_0\lambda^2}\int_0^{2\pi}d\theta_1\int_0^{2\pi}d\theta_2\frac{\cos(\theta_1-\theta_2)}{\left|\sin\frac{\theta_1-\theta_2}{2}\right|}\times\theta\left(2x_0\left|\sin\frac{\theta_1-\theta_2}{2}\right|-\xi\right). \tag{14}$$

Compared to F_v, the stray term is negligibly small, $F_s\sim\frac{\phi_0^2}{\mu_0\lambda}(\frac{x_0}{\lambda})^2$. The interaction energy with the external current reads

$$F_{\mathrm{ext}}(x_0)=-\frac{I\phi_0 x_0^2}{2\lambda^2}\tilde{f}(d/\lambda),$$

$$\tilde{f}(x)=\int_0^\infty dy e^{-yx}(\sqrt{y^2+1}-y). \tag{15}$$

Using these formulas for F_v and F_{ext} we obtain from Eq. (13) the estimate

$$I_S\sim\frac{\phi_0}{8\mu_0\xi\tilde{f}(d/\lambda)}. \tag{16}$$

The dependence of I_S on d/λ is hidden in the function $\tilde{f}(x)$, with $\tilde{f}(x\to\infty)\to x^{-1}$ and $\tilde{f}(x\to 0)\to\log(x^{-1/2})+c$, where $c\sim 0.3$. For $d\gg\lambda$ we have $I_S\sim\frac{\phi_0 d}{8\mu_0\xi\lambda}$. In this case the magnetic field due to the external current at $x=z=0$ is $[H_0(\vec{r}=0)]_z\to\frac{I_S}{\pi d}$. It is of the order of the second critical field H_{c2}. In the other limit $d\ll\lambda$ we have $I_S\sim\frac{\phi_0}{4\mu_0\xi\log[\lambda/d]}$. Note that this behavior holds for $\xi\ll d\ll\lambda$. In this regime we have $I_S\gg I_{c1}\sim\frac{\phi_0}{\mu_0\lambda}$. In Fig. 10 we plot the phase diagram of the system.

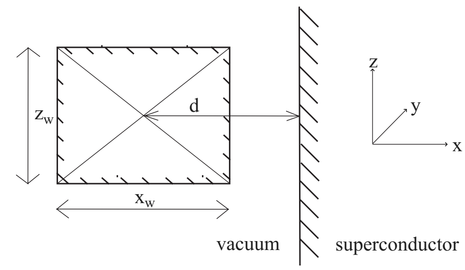

FIG. 11. Rectangular cross section of the wire carrying the external current.

B. Finite wire cross section

To make connection with experiment we consider a finite cross section of the wire carrying the external current. Consider the rectangular cross section as shown in Fig. 11 and assume that the current I flows uniformly in this cross section.

We can write the external current density as

$$\vec{j}_{\mathrm{ext}}\to-\frac{I}{x_w z_w}\int_{d-x_w/2}^{d+x_w/2}d\tilde{d}\int_{-z_w/2}^{z_w/2}d\tilde{z}\,\delta(x-\tilde{d})\delta(z-\tilde{z})\hat{y}. \tag{17}$$

The modification to the magnetic field $\vec{H}=\vec{H}_0+\vec{H}_v+\vec{H}_s$ occurs only in the first term,

$$\vec{H}_0(\vec{r})\to\frac{1}{x_w z_w}\int_{d-x_w/2}^{d+x_w/2}d\tilde{d}\int_{-z_w/2}^{z_w/2}d\tilde{z}[\vec{H}_0(x,y,z-\tilde{z})]_{d\to\tilde{d}},$$

where $\vec{H}_0(x,y,z)$ is given in Eq. (4). Next we focus on the modification of the vortex-dependent part of the free energy $F=F_v+F_s+F_{\mathrm{ext}}$. Only the term F_{ext} is modified. Using Eq. (17) it is easy to find that

$$F_{\mathrm{ext}}\to-\frac{I\phi_0}{\pi}\int_\Gamma d\vec{r}_z\int_0^\infty dk e^{-kd}\cos(kr_z)(1-e^{-\tau(k)r_x})\times\left(1-\frac{k}{\tau(k)}\right)\left(\frac{\sinh\frac{kx_w}{2}}{\frac{kx_w}{2}}\frac{\sin\frac{kz_w}{2}}{\frac{kz_w}{2}}\right). \tag{18}$$

Let us first specialize to the case of square cross section where the wire touches the SC, $x_w=z_w=2d$, and compare this with a pointlike cross section $x_w=z_w\to 0$ (we ignore any electron or Cooper pair tunneling between the SC and wire). We have repeated the calculation of I_{c0} and I_{c1}. The results are roughly the same for both cross sections for $d\lesssim\lambda$, and deviations up to 10% are obtained for $d\gg\lambda$ up to $d=100\lambda$. In Fig. 12 we compare the contours at I_{c1} as a function of d for the two cross sections. We can see that z_0 changes by a factor of ≤ 1.6 for $d\leq 90\lambda$.

The magnetic field at the surface just below I_{c1} is compared for the two cross sections in Fig. 13. At $d\gg\lambda$ it approaches H_{c1} in both cases, while for $d\ll\lambda$ it is larger for pointlike cross section by about 10%.

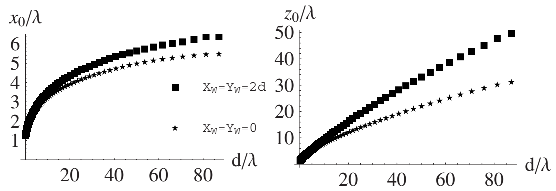

FIG. 12. d dependence of x_0 and z_0 for two cross sections of the wire.

Next we consider the dependence on z_w for $z_w \geq x_w = 2d$ which can be experimentally relevant. The limit $z_w \to \infty$ can be treated analytically since the external field $\vec{H}_0$ is uniform at all $x > (-d + \frac{x_w}{2})$. In this limit $H_{\text{surface}}(I_{c1}) \to H_{c1}$. For finite z_w we calculated $H_{\text{surface}}(I_{c1})$ numerically, see Fig. 14. We conclude that z_w should not be too large in order to obtain a sizable enhancement of the surface field in the vortex-free state for a disordered surface.

We estimate the typical value of the threshold current I_{c1}. For the regime of interest $d \sim \lambda$, we have $I_{c1} \sim \frac{\phi_0}{\mu_0 \lambda} = \frac{1.6455\ \text{mA}}{\lambda[\mu\text{m}]}$. For $\lambda = 1\ \ \mu$m this corresponds to current density of $\sim 1\ \ \text{mA}\ \mu\text{m}^{-2}$.

IV. CONCLUSIONS

In this work we studied solutions of London theory in a geometry where an external mesoscopic current flows parallel to a surface of a SC. Only above the threshold current I_{c0} do there exist solutions with curved flux lines entering and leaving the SC at the surface. At a larger threshold current, I_{c1}, these solutions become energetically favorable; however an energy barrier separates them from the vortex-free solution. At a third threshold current, I_S, this barrier disappears. To determine the current at which vortices actually penetrate the sample, one has to account for the degree of disorder of the surface. For strong surface disorder the vortex can penetrate at $I = I_{c1}$ despite the presence of the barrier due to large local magnetic fields produced at impurity sites allowing for nucleation of vortices. On the other hand, for a clean surface, the entrance of vortices occurs at $I = I_S$.

By calculating those currents using a numerical solution of the problem we conclude that for strong surface disorder, the present geometry allows one to achieve locally larger magnetic fields in the vortex-free state, as compared to the case of homogeneous magnetic field, provided that the wire thickness is of O(λ). This can be potentially relevant for experiments in high-temperature superconductors which typically have extremely low values of H_{c1}. We argued that the effect of enhancement of the magnetic field in the vortex-free (Meissner) state becomes more pronounced in strongly anisotropic superconductors, which is particularly relevant for layered high-temperature superconductors.

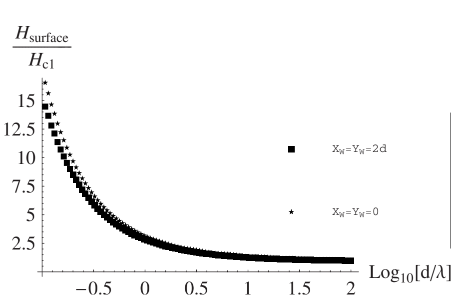

FIG. 13. Magnetic field at the surface (see definition in text) just before the entry of the first vortex at $I \to I_{c1}$ for either zero wire cross section ($x_x = z_w = 0$, stars) or finite cross section ($x_x = z_w = 2d$, squares).

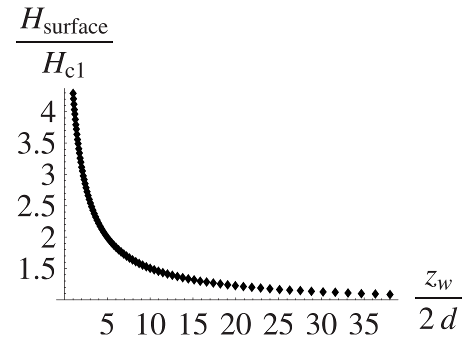

FIG. 14. Magnetic field at the surface at $I \to I_{c1}$ as a function of z_w for $x_w = 2d$ and $d = \lambda/2$.

ACKNOWLEDGMENTS

We would like to thank Jordan Baglo, Walter Hardy, and Cedric Lin for stimulating discussions. This work was supported by NSERC (E.S. and I.A.) and CIfAR (I.A.).

APPENDIX: MIXED TERMS IN FREE ENERGY

We shall prove the vanishing of crossed term in the energy Eq. (1) between $\vec{H}_0$ and $\vec{H}_s$ [see Eq. (4)],

$$F_{(H_0 H_s)} = \mu_0 \int d^3 r [\vec{H}_0 \cdot \vec{H}_s + \theta(x) \lambda^2 (\vec{\nabla} \times \vec{H}_0) \cdot (\vec{\nabla} \times H_s)] = 0. \tag{A1}$$

From Eq. (4) we have $\vec{H}_0 = \vec{H}_0' + \vec{H}_{s0}$ where $\vec{H}_0' = \theta(-x)(\vec{H}_{I,d} + \vec{H}_{-I,-d}) = \vec{\nabla} \times \vec{A}_1$ and

$$\vec{A}_1 = \frac{I\hat{y}}{4\pi} \log \frac{(x+d)^2 + z^2}{(x-d)^2 + z^2}, \quad x < 0. \tag{A2}$$

Correspondingly, we have $F_{(H_0 H_s)} = F_{(H_0' H_s)} + F_{(H_{s0} H_s)}$. Consider the term $F_{(H_0' H_s)} = \mu_0 \int_{x<0} d^3 r \vec{H}_0' \cdot \vec{H}_s$. We will use the vector identity $(\vec{\nabla} \times \vec{A}) \cdot \vec{B} = \vec{A} \cdot (\vec{\nabla} \times \vec{B}) + \vec{\nabla} \cdot (\vec{A} \times \vec{B})$, with $\vec{A} = \vec{A}_1$, $\vec{B} = \vec{H}_s$, and the fact that $\vec{\nabla} \times \vec{H}_s = 0$. Then the volume integral can be transformed to an integral on the surface $x = 0^-$. However this integral vanishes because $\vec{A}_1(0^-, y, z) = 0$, hence $F_{(H_0' H_s)} = 0$. Now let us consider the term $F_{(H_{s0} H_s)}$ and define $\vec{H}_s = \vec{\nabla} \times \vec{A}_s$. For the integral in the region $x < 0$ we use the above vector identity with $\vec{A} = \vec{A}_s$ and $\vec{B} = \vec{H}_{s0}$, and for $x > 0$ we use the vector identity with $\vec{A} = \vec{H}_{s0}$ and $\vec{B} = \vec{\nabla} \times \vec{H}_s$.

Taking into account that $\vec{H}_s$ and $\vec{H}_{s0}$ satisfy the homogeneous equations, we obtain

$$\int_{x<0} d^3r(\vec{\nabla}\times\vec{A}_s)\cdot\vec{H}_{s0} = \int dS(\vec{A}_s^- \times \vec{H}_{s0}^-)_x,$$

$$\int_{x>0} d^3r[\vec{H}_{s0}\cdot\vec{H}_s + \lambda^2(\vec{\nabla}\times\vec{H}_{s0})\cdot(\vec{\nabla}\times H_s)] = -\lambda^2\int dS[\vec{H}_{s0}^+ \times (\vec{\nabla}\times\vec{H}_s^+)]_x. \tag{A3}$$

Here $\int dS = \int_{-\infty}^{\infty}dy\int_{-\infty}^{\infty}dz$ and $\vec{H}^\pm = \vec{H}(x=0^\pm, y, z)$. For $x>0$ we can use $\vec{A}_s = -\lambda^2\vec{\nabla}\times\vec{H}_s$, which follows from the London equation for $\vec{H}_s$. Next we use the fact that by construction, $\vec{H}_s^- = \vec{H}_s^+ + \vec{H}_v^+$. This allows us to express $\vec{A}_s^- = -\lambda^2\vec{\nabla}\times(\vec{H}_v^+ + \vec{H}_s^+)$ and combine the two terms of Eq. (A3) as

$$F_{(H_{s0}H_s)} = -\mu_0\lambda^2\int dS[(\vec{\nabla}\times\vec{H}_s^+)\times(\vec{H}_{s0}^- - \vec{H}_{s0}^+) + (\vec{\nabla}\times\vec{H}_v)^+ \times \vec{H}_{s0}^-]_x. \tag{A4}$$

Now we use the explicit forms of these factors $(\vec{H}_{s0}^- - \vec{H}_{s0}^+) = -\frac{Id\hat{z}}{\pi(d^2+z^2)}$, $(\vec{H}_{s0}^-)_y = 0$,

$$(\vec{\nabla}\times\vec{H}_s^+)_y = -\frac{\phi_0}{2\mu_0\lambda^2}\int_\gamma d\vec{r}_x'\int\frac{d^2k_2}{(2\pi)^2}e^{-i\vec{k}_2\cdot\vec{r}' + i(k_y y + k_z z) - \tau(k_2)|\vec{r}_x'|} \times \frac{-ik_z[\tau(k_2)-k_2]}{k_2\tau(k_2)},$$

$$(\vec{\nabla}\times\vec{H}_v^+)_y = \frac{\phi_0}{2\mu_0\lambda^2}\int_\gamma d\vec{r}_x'\int\frac{d^2k_2}{(2\pi)^2}e^{-i\vec{k}_2\cdot\vec{r}' + i(k_y y + k_z z) - \tau(k_2)|\vec{r}_x'|} \times \frac{ik_z}{\tau(k_2)}\left(1 - \frac{\tau^2(k_2)}{k_z^2}\right),$$

$$(\vec{H}_{s0}^-)_z = -I\int\frac{d^2k_2}{(2\pi)^2}e^{i\vec{k}_2\cdot\vec{r} - |k_z|d}\frac{k_2 2\pi\delta(k_y)}{\tau(k_2)+k_2}. \tag{A5}$$

Plugging these expressions in Eq. (A4), one can readily obtain $F_{(H_{s0}H_s)} = 0$ (without performing any integration), completing the proof for $F_{(H_0 H_s)} = 0$.

[1] C. P. Bean and J. D. Livingston, Phys. Rev. Lett. **12**, 14 (1964).
[2] P. G. De Gennes, *Superconductivity of Metals and Alloys* (Benjamin, New York, 1966).
[3] A. S. Joseph and W. J. Tomasch, Phys. Rev. Lett. **12**, 219 (1964).
[4] R. W. De Blois and W. De Sorbo, Phys. Rev. Lett. **12**, 499 (1964).
[5] M. Konczykowski, L. I. Burlachkov, Y. Yeshurun, and F. Holtzberg, Phys. Rev. B **43**, 13707 (1991).
[6] J. K. Gregory, M. S. James, S. J. Bending, C. J. van der Beek, and M. Konczykowski, Phys. Rev. B **64**, 134517 (2001).
[7] R. Liang, P. Dosanjh, D. A. Bonn, W. N. Hardy, and A. J. Berlinsky, Phys. Rev. B **50**, 4212 (1994).
[8] E. Zeldov, A. I. Larkin, V. B. Geshkenbein, M. Konczykowski, D. Majer, B. Khaykovich, V. M. Vinokur, and H. Shtrikman, Phys. Rev. Lett. **73**, 1428 (1994).
[9] E. H. Brandt, Phys. Rev. B **60**, 11939 (1999).
[10] N. Morozov, E. Zeldov, M. Konczykowski, and R. A. Doyle, Physica C **291**, 113 (1997).
[11] F. London, *Superfluids* (Wiley, New York, 1950), Vol. I, Sec. VIII.
[12] J. Bok and J. Klein, Phys. Rev. Lett. **20**, 660 (1968).
[13] J. B. Brown and T. D. Morris, Proceedings of the 11th International Conference on Low Temperature Physics, edited by J. F. Allen, D. M. Finlayson, and D. M. McCall (St. Andrews University Press, Fife, Scotland, 1968), Vol. 2, p. 768.
[14] T. D. Morris and J. B. Brown, Physica (Amsterdam) **55**, 760 (1971).
[15] P. Lipavský, K. Morawetz, J. Koláček, J. J. Mareš, E. H. Brandt, and M. Schreiber, Phys. Rev. B **70**, 104518 (2004).
[16] G. Blatter and V. Geshkenbein, Phys. Rev. B **47**, 2725 (1993); E. H. Brandt, *ibid.* **48**, 6699 (1993).
[17] A. Sudbø, E. H. Brandt, and D. A. Huse, Phys. Rev. Lett. **71**, 1451 (1993).
[18] E. H. Brandt, J. Low Temp. Phys. **42**, 557 (1981).
[19] L. N. Shehata and A. G. Saif, J. Low Temp. Phys. **56**, 113 (1984).